Aquatic Toxicology 191 (2017) 105–112

Contents lists available at ScienceDirect

Aquatic Toxicology

journal homepage: www.elsevier.com/locate/aqtox

Research Paper

Time-gated luminescence imaging of singlet oxygen photoinduced by fluoroquinolones and functionalized graphenes in *Daphnia magna*

Tianlie Luo[a], Jingwen Chen[a,*], Bo Song[b,*], Hua Ma[b], Zhiqiang Fu[a], Willie J.G.M. Peijnenburg[c,d]

[a] Key Laboratory of Industrial Ecology and Environmental Engineering (MOE), School of Environmental Science and Technology, Dalian University of Technology, Linggong Road 2, Dalian 116024, China
[b] State Key Laboratory of Fine Chemicals, School of Chemistry, Dalian University of Technology, Linggong Road 2, Dalian 116024, China
[c] Institute of Environmental Sciences, Leiden University, 2300 RA Leiden, The Netherlands
[d] National Institute of Public Health and the Environment, Center for the Safety of Substances and Products, 3720 BA Bilthoven, The Netherlands

ARTICLE INFO

Keywords:
Singlet oxygen
Fluoroquinolones
Functionalized graphene
Daphnia magna
Time-gated luminescence imaging

ABSTRACT

Singlet oxygen ($^1O_2$) can be photogenerated by photoactive xenobiotics and is capable of causing adverse effects due to its electrophilicity and its high reactivity with biological molecules. Detection of the production and distribution of $^1O_2$ in living organisms is therefore of great importance. In this study, a luminescent probe ATTA-Eu^{3+} combined with time-gated luminescence imaging was adopted to detect the distribution and temporal variation of $^1O_2$ photoinduced by fluoroquinolone antibiotics and carboxylated/aminated graphenes in *Daphnia magna*. Results show that the xenobiotics generate $^1O_2$ in living daphnids under simulated sunlight irradiation (SSR). The photogeneration of $^1O_2$ by carboxylated/aminated graphenes was also confirmed by electron paramagnetic resonance spectroscopy. The strongest luminescence signals of $^1O_2$ were observed in the hindgut of daphnids, and the signals in different areas of the daphnids (gut, thoracic legs and post-abdominal claw) displayed a similar trend of enhancement over irradiation time. Mean $^1O_2$ concentrations at different regions of daphnids within one hour of SSR irradiation were estimated to be in the range of 0.5 ~ 4.8 μM. This study presented an efficient method for visualizing and quantifying the temporal and spatial distribution of $^1O_2$ photogenerated by xenobiotics in living organisms, which can be employed for phototoxicity evaluation of xenobiotics.

1. Introduction

Singlet oxygen ($^1O_2$), the lowest electronic excited state of molecular oxygen, has both electrons in a same molecular orbital with paired spins (Jensen et al., 2011). Due to its electrophilicity, $^1O_2$ can react with organic molecules containing electron-rich functional groups or double bonds, e.g. biological molecules (proteins, DNA bases, lipids, sterols, amino acids, and peptides) (Ogilby, 2010; DeRosa and Crutchley, 2002; Davies, 2003; Wilkinson et al., 1993). Due to its reactivity, $^1O_2$ also plays a vital role in inactivation of viruses and bacteria since it is capable of causing site-specific amino acid oxidation in virus protein capsids, and damage to membrane-bound proteins by oxidative stress and carbonylation (Kohn and Nelson, 2007; Kohn et al., 2007).

$^1O_2$ can be produced in a variety of ways, among which photosensitized generation involving energy transfer from an excited state of a sensitizer to $^3O_2$, has aroused widespread concern (Ogilby, 2010; Latch and McNeill, 2006). It is known that dissolved organic matter and several classes of organic chemicals/pollutants (e.g. aromatic hydrocarbons, organic dyes, drugs, phenols, quinones, metal oxide nanoparticles, fullerenes, carbon nanotubes) can generate $^1O_2$ under irradiation (DeRosa and Crutchley, 2002; Wilkinson et al., 1993; Redmond and Gamlin, 1999; Latch and MaNeill, 2006; Yin et al., 2008; Ray et al., 2002; Hotze et al., 2008, 2009; Li et al., 2012; Santaella et al., 2014; Zhao et al., 2008; Bagrov et al., 2015; Chen and Zepp, 2015). Wilkinson et al. (1993) reviewed the quantum yields for the photosensitized formation of $^1O_2$ in solutions, while Redmond and Gamlin (1999) compiled $^1O_2$ yields from biologically relevant molecules (e.g. angelicins, DNA and related compounds, quinones, retinoids).

Abbreviations: $^1O_2$, singlet oxygen; SSR, simulated sunlight irradiation; ROS, reactive oxygen species; ATTA-Eu^{3+}, [4′-(9-anthryl)-2,2′: 6′,2″-terpyridine-6,6″-diyl)]bis(methylenenitrilo) tetrakis(acetate)-Eu^{3+}; TEMP, 2,2,6,6-Tetramethyl-4-piperidone; LOM, lomefloxacin; EPR, electron paramagnetic resonance; CIP, ciprofloxacin; Gr-COOH, carboxylated graphene; Gr-NH_2, aminated graphene; PBS, phosphate buffer saline; Lumin, luminescence; ATLI;, ATTA-Eu^{3+} probe combined the time-gated luminescence imaging; MMP-1, matrix metalloproteinase-1; HO-1, heme oxygenase-1; ICAM-1, intercellular adhesion molecule-1

* Corresponding authors.
E-mail addresses: jwchen@dlut.edu.cn (J. Chen), bo.song@dlut.edu.cn (B. Song).

http://dx.doi.org/10.1016/j.aquatox.2017.07.016
Received 5 May 2017; Received in revised form 26 July 2017; Accepted 27 July 2017
Available online 29 July 2017
0166-445X/

In biological systems, excess $^1O_2$ photogenerated by exogenous pollutants is a mechanism of photoinduced toxicity as $^1O_2$ can react with various biological molecules, causing damage and leading to cell death (Yin et al., 2008; Zhao et al., 2008, 2009; Mujtaba et al., 2013; Fischer et al., 2004; Gocke et al., 1998; Rancan et al., 2002). However, due to its high reactivity and short lifetime, the diffusion distance of $^1O_2$ is only about 10 nm in a physiologically relevant situation (DeRosa and Crutchley, 2002). Hence, $^1O_2$ photoinduced by different pollutants localized in different cellular compartments can only interact with molecules mostly in its nearest environment. As a result, the production site of $^1O_2$ is a key factor for assessing $^1O_2$ induced detrimental processes. For instance, the malonic acid C_{60} tris-adduct was found to be more phototoxic to Jurkat cells than the dendritic C_{60} mono-adduct because the former was postulated to associate closer with the biological target even though its $^1O_2$ quantum yield was lower (Rancan et al., 2002). Thus, it is of importance to investigate the production and distribution of $^1O_2$ photoinduced by exogenous pollutants in living organisms.

To the best of our knowledge, there have been just a few studies investigating the generation and distribution of $^1O_2$ photoinduced by organic pollutants in living organisms. The short lifetime of $^1O_2$ in biological systems makes it difficult to detect $^1O_2$. Additionally, the energy transfer process for $^1O_2$ generation usually competes with electron transfer reactions. The generation process of $^1O_2$ by photosensitizers may thus accompany the generation of other reactive oxygen species (ROS) during irradiation (Ogilby, 2010). Therefore, rapid, sensitive, and readily available techniques for detecting the production and distribution of $^1O_2$ in living organisms are needed.

Time-gated fluorometry combined with lanthanide complex-based luminescence probes has emerged as a good method for $^1O_2$ detection in biological systems such as Hela cells and HepG2 cells (Sun et al., 2015; Song et al., 2005a, 2005b, 2006). For example, the almost non-luminescent chelate ATTA-Eu^{3+} (Fig. 1) can specifically react with $^1O_2$ and form an endoperoxide (EP-ATTA-Eu^{3+}) with strong phosphorescence intensity that can be detected by time-gated luminescence measurement. Compared with other $^1O_2$ responsive probes, the ATTA-Eu^{3+} probe possesses properties of long luminescence lifetime, large Stokes shift and a sharp emission profile, which makes it suitable for use in microsecond time-gated luminescence measurements in which the interference caused by background noises associated with biological samples, scattering lights and optical components is minimized (Song et al., 2005a). Thus, the ATTA-Eu^{3+} probe may be useful for luminescence detection of $^1O_2$ in living organisms.

In this study, the feasibility of using the ATTA-Eu^{3+} probe to detect the production and distribution of $^1O_2$ photogenerated by photoactive chemicals in *Daphnia magna* was tested. *D. magna* was selected because it plays an important role in the aquatic food chain, and is a representative of aquatic invertebrates and a model organism in ecotoxicity testing (Du et al., 2016; Li et al., 2016b). Two types of photoactive chemicals were selected for the study, fluoroquinolones (lomefloxacin, ciprofloxacin) and functionalized graphenes (carboxylated or aminated graphenes). Fluoroquinolone antibiotics have been observed to photogenerate $^1O_2$ in water systems (Albini and Monti, 2003; Martinez et al., 1998). As sunlight-induced $^1O_2$ production by fullerene, fullerol and carbon nanotubes has been observed (Zhao et al., 2008; Bagrov et al., 2015; Chen and Zepp, 2015), we hypothesized that functionalized graphenes that can readily be dispersed in aqueous solutions, can also photogenerate $^1O_2$. Specifically, using the time-gated luminescence imaging technology, the real-time production and distribution of $^1O_2$ in *D. magna* during irradiation were visualized and quantified.

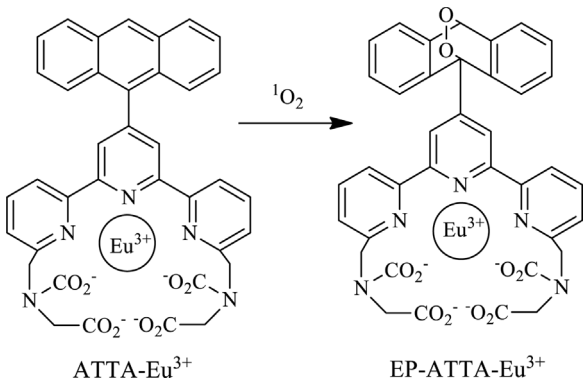

Fig. 1. Reaction of ATTA-Eu^{3+} with $^1O_2$.

2. Materials and methods

2.1. Chemicals and reagents

Lomefloxacin (CAS: 98079-51-7, 98%), ciprofloxacin (CAS: 85721-33-1, 98%) and 2,2,6,6-Tetramethyl-4-piperidone (TEMP, CAS: 826-36-8, 99%) were purchased from J & K Scientific Ltd (Beijing, China). Carboxylated graphene (Gr-COOH) and aminated graphene (Gr-NH_2) were supplied by Nanjing XFNANO Materials Tech Co., Ltd (Nanjing, China). The organic ligand of the $^1O_2$ probe, ATTA, [4′-(9-anthryl)-2,2′:6′2″-terpyridine-6,6″-diyl)]bis(methylenenitrilo) tetrakis(acetate) was synthesized as reported in a previous study (Song et al., 2005). The stock solution of ATTA-Eu^{3+} was prepared by in situ mixing of equivalent molar amounts of ATTA (0.5 mM) and $EuCl_3{\cdot}6H_2O$ (0.5 mM) into 0.02 M phosphate buffer saline (PBS) at pH 7.4. Other reagents (purity > 99.0%) were purchased from Kermel Chemical Reagent Co., Ltd (Tianjin, China). Ultrapure water was obtained with an OKP ultrapure water system (Shanghai Lakecore Instrument Co., China).

2.2. Test organisms

Daphnia neonates (< 1 day old) used in the bioassays were offspring from an in-house laboratory stock maintained in an artificial climate incubator at 20 ± 1 °C with a photoperiod of 16:8 h light/dark. The daphnids were fed with a culture of green algae (*Scenedesmus sp.*) once a day. All the tests were carried out in reconstituted water (detailed in the supplementary data, Table S1) aerated for more than three days. During the exposure and bioassay experiments, the daphnids were not fed.

2.3. Preparation and characterization of functionalized graphene suspensions

To obtain a stable dispersion, Gr-COOH and Gr-NH_2 were suspended in pure water (18 MΩ cm) and subjected to ice-bath sonication for 2 h at 200 W. After sonication, the solutions were filtered through a 0.45 μm polytetra fluoroethylene membrane to remove undissolved particles and the filtrates were stored in brown glass bottles in the dark. A total organic carbon analyzer (Multi N/C 2100S, Analytikjena, Germany) was used to indicate the concentration of the functionalized graphenes in the stock solutions.

Particle size distributions and zeta potentials of the Gr-COOH and Gr-NH_2 suspensions were determined by dynamic light scattering using a Malvern particle size analyzer (Nano-ZS90, Worcestershire, UK). The morphology and thickness of the particles were observed by atomic force microscopy (PicoScan 2500, Molecular Imaging, America). Fourier transformed infrared spectroscopy (EQUINOX 55, Bruker, America) and Raman spectroscopy (DRX, Thermo Fisher Scientific, America) were used to analyze surface functional groups. The absorption peaks of Gr-COOH and Gr-NH_2 were characterized by a UV–vis spectrophotometer (UV2900, Hitachi, Japan). The characteristics of the Gr-COOH and Gr-NH_2 are detailed in the supplementary data (Table S2, Fig. S1-S5).